Adsorption properties in high optical quality nanoZIF-8 thin films with tunable thickness†

Aude Demessence,[ab] Cédric Boissière,[a] David Grosso,[a] Patricia Horcajada,[b] Christian Serre,*[b] Gérard Férey,[b] Galo J. A. A. Soler-Illia[c] and Clément Sanchez*[a]

Received 24th February 2010, Accepted 25th June 2010
DOI: 10.1039/c0jm00500b

We report processing of a thin film by chemical solution deposition of a microporous ZIF-8 nanoparticle dispersion. By using the drain and capillary regimes involved in the dip-coating process, we tuned the thickness of the films from 40 nm to 1 μm and controlled the packing of the nanoparticles on the substrate. The high optical quality thin films show a dual hierarchical porous structure from the micropores of the framework and the mesoporous interparticular voids. Moreover, vapor sorption properties of the microporous ZIF-8 based thin films have been evaluated by ellipsometric porosimetry. The hydrophobic films show alcohol, THF and hydrocarbon adsorption. Experiments for isopropanol/water separation have been carried out and the selective adsorption of the alcohol *versus* the water makes these thin films good candidates for vapor sensors.

Introduction

In the last decade Metal–Organic Frameworks (MOFs) have emerged as a fascinating class of porous materials due to their potential applications in different domains such as gas sorption, storage, separation, drug release, optics and catalysis.[1] Nevertheless, to open the way to applications such as membranes, pellets, extrudates, packed columns, functional coatings, sensors or patches, a real effort has to be made on shaping the hybrid materials. Since 2005, few groups have studied the processing of thin films of MOFs using different approaches.[2] The first route, involves the direct crystal growth/deposition from solvothermal mother solutions which results in more or less densely packed films of intergrown crystallites of micrometric sizes.[3] A recent control of the seeding made it possible to successfully prepare a roughly 2 μm thick ZIF-7 membrane on α-alumina support wherein it showed good efficiency in the separation of hydrogen from carbon dioxide.[4] The second method, a stepwise layer-by-layer growth onto a substrate, offers homogeneous highly oriented films, however it requires self-assembled monolayer substrates and a long repetitive process of immersion/washing cycles.[5] Even if the first approach, which leads to films with a high roughness, is applied for supported membranes, applications of MOF-based films in nanotechnology, or microelectronics, sensors, smart membranes, transparent protective or catalytic coatings then require thin films with high optical quality. Among different known techniques of deposition leading to high optical quality thin films, such as chemical vapor deposition (CVD), molecular beam epitaxy (MBE) or atomic layer deposition (ALD), chemical solution deposition (CSD) (also known as spin coating or dip coating) remains the fastest, simplest and cheapest technique to obtain excellent control over the thickness. The CSD techniques are also widely used at laboratory level and in industry due to their low-cost and the possibility of large-area processing. In order to process thin films of MOFs of high optical quality, we have recently initiated another approach which consists of the chemical solution deposition of preformed nanoparticles (NPs) of MOFs on a bare surface.[6] In addition to the transparency of the films and the easy deposition processing, this route offers several advantages such as the control of the particle size for a better diffusion of adsorbed molecules and the presence of well-defined grain boundaries (which is typically hard to control for usual crystal growing) leading to multi-pore size film systems. This led recently to high optical quality thin films of two carboxylate-based MOFs, a rigid chromium terephthalate MIL101(Cr) and a flexible iron muconate MIL89(Fe) materials.[6] The water adsorption studies of MIL101(Cr) material led to the characterization of a well-defined hierarchical porosity associated to the two different pore sizes of the MOF and the interparticular void. The MIL-89 system showed a reversible breathing of the films upon water vapor adsorption associated to the flexible structure. To extend this approach to different systems, here we report the process of high optical quality thin films of microporous ZIF-8 (ZIF = zeolitic imidazolate frameworks). ZIF-8 exhibits a cubic architecture that can be described by a space-filling packing of regular truncated octahedra (Scheme 1). This defines 1.2 nm diameter pores connected *via* 0.35 nm diameter apertures (6-membered rings), the 4-membered rings being too small for the guest molecules to go through. This resulting highly porous structure has a Brunauer-Emmett-Teller (BET) surface area close to 1800 $m^2\ g^{-1}$.[7] According to the deposition conditions of the colloidal solution, the thickness of ZIF-8 thin films can be tuned

[a]*Laboratoire de Chimie de la Matière Condensée de Paris, UMR CNRS 7574, Collège de France, Université Paris 6, France. E-mail: clement.sanchez@upmc.fr.; Tel: +33 144271501*
[b]*Institut Lavoisier, UMR CNRS 8180, Université de Versailles, St Quentin-en-Yvelines, France. E-mail: serre@chimie.uvsq.fr.; Tel: +33 139254304*
[c]*Gerencia de Química, CNEA, Centro Atómico Constituyentes, Av. Gral Paz 1499, San Martín, B1650KNA, Argentina*
† Electronic Supplementary Information (ESI) available: Characterizations of NPs (DLS, MET, N_2 adsorption), of the films (photos, UV–vis, IR) and evolution of the thickness and refractive index of thin films upon vapor adsorption. See DOI:10.1039/c0jm00500b

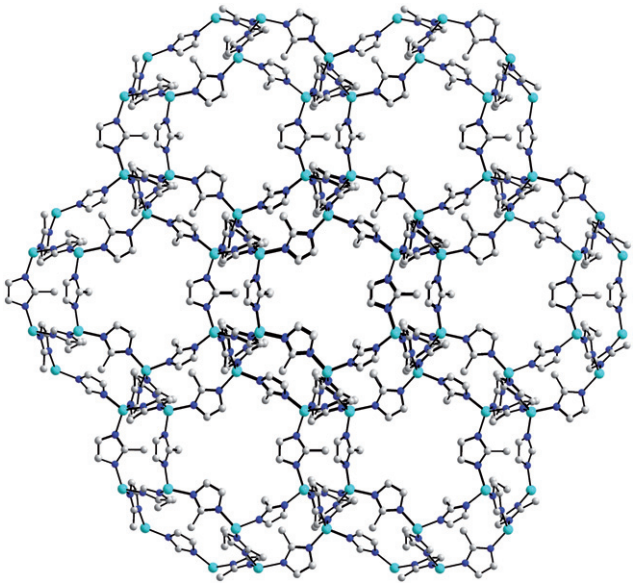

Scheme 1 View of the crystal structure of ZIF-8 showing the six-membered ring one-dimensional channels along the [111] direction. Cyan, blue, and grey spheres represent Zn, N, and C atoms, respectively. H atoms are omitted for clarity.

between 40 nm to 1 μm, pointing to the easiness of the CSD to control the film thickness, which is hard to predict by using a direct crystallites growth on a substrate in solvothermal conditions.[8] The vapor adsorption properties of the ZIF-8 thin films and their potential as sensors are also described here.

Experimental

Synthesis of the colloidal solution

The synthesis of the nanoparticles followed the conditions previously reported by Cravillon *et al.*[9] A solution of $Zn(NO_3)_2 \cdot 6H_2O$ (2.933 g, 9.87 mmol; 98% Sigma-Aldrich) in 200 mL of methanol (Aldrich, 99%) is rapidly poured into a solution of 2-methylimidazole (Hmim; 6.489 g, 79.04 mmol; 99% Aldrich) in 200 mL of methanol under vigorous stirring at room temperature. The mixture slowly turns turbid and after 1 h the nanocrystals are separated from the milky dispersion by centrifugation at 20000 rpm for 15 min. To remove the excess of unreacted acid and zinc nitrate species, ZIF-8 nanoparticles were readily redispersed in absolute ethanol and centrifuged. Three washing cycles of the redispersion in absolute EtOH/centrifugation were carried out to get the calculated surface area of ZIF-8 material. For powder analyses, the particles were dried under vacuum and for thin film deposition, the particles were left in absolute ethanol, yielding stable colloidal dispersions from which sedimentation does not occur for three weeks.

Preparation of the thin films

Thin films were prepared by dip-coating a freshly washed colloidal solution of ZIF-8 NPs (nanoparticles) at room temperature under ambient atmospheric conditions, using single-side polished silicon wafers previously washed with acetone. Films were deposited at withdrawal speeds ranging from 0.01 to 10 mm s^{-1}. The whole dip-coater was isolated from natural vibration and external convection to prevent the formation of horizontal strips associated with the fluctuation of the solution surface that creates meniscus instability. The use of a solution container allowing only a minimal fraction of the solution to interface with air is required and used in this experiment. These controls are necessary for ultra-low withdrawal speeds. After NPs deposition, the films were maintained for two additional minutes under ambient conditions before being heated at 130 °C for five min in air, washed with ethanol and dried again at 130 °C in air. This did not affect the final structure. Increasing the film thickness in the drain regime was achieved through multiple depositions with the same washing conditions.

Characterization

The X-ray powder diffraction patterns were collected in a conventional high resolution (θ–2θ) D5000 Siemens X'Pert MDP diffractometer (λ_{Cu} Kα_1, Kα_2) from 2 to 30° (2θ) using a step of 0.02° and 10 s per step in continuous mode. Grazing-incidence wide-angle X-ray scattering (GI-WAXS) was recorded using a Rigaku S-MAX 3000 with simultaneous small angle X-ray scattering (SAXS) capabilities, on an image plate. Infrared spectra were collected with a Nicolet Magna 550 spectrometer with ATR. Transmission electron microscopy (TEM) was carried out using a JEOL 100 CX II microscope. TEM micrographs were processed with a slow scan CCD camera and analyzed with the Digital Micrograph program. FESEM images of the films were taken with a ZEISS LEO 982 GEMINI field emission electron microscope in the secondary electron mode using an in-lens detector to improve resolution. The nitrogen sorption experiments were performed at 77 K on a Micromeritics ASAP 2010 sorption analyzer after activation of the sample (*ca.* 0.05 g) at 120 °C for 12 h under primary vacuum. Dynamic light scattering and zeta potential experiments were performed using a Malvern nanosizer (Nano ZS) at 173°. Ellipsometry measurements were carried out on a UV–visible (240–1000 nm) Variable Angle Spectroscopic Ellipsometer (VASE) from Woolam, and the data analysis was performed with the WVase 32 software. The thickness of the film was deduced from the UV–vis spectroscopic ellipsometry measurements, using the Cauchy model of optical dispersion in non-absorbing regions of the spectrum (450–1000 nm). Environmental ellipsometry porosimetry involves a dynamic *in situ* monitoring of the refractive index and the thickness of the film upon variation of the relative vapor pressures between 0% and 100% inside the analysis chamber.[10]

Results and discussion

Synthesis of the nanoparticles of ZIF-8

The first step before film processing consists of preparing a stable and homogenous colloidal solution of the rigid microporous ZIF-8. For that we followed the synthesis conditions of the ZIF-8 nanoparticles previously reported, at room temperature for 60 min, leading to monodisperse and non-aggregated NPs of size with a *Z*-average of 28 ± 15 nm and a polydispersity index of 0.083 nm as determined by dynamic light scattering (Fig. S1) and transmission electronic microscopy (Fig. S2). X-Ray powder diffraction pattern (XRPD) shows the characteristic Bragg peaks

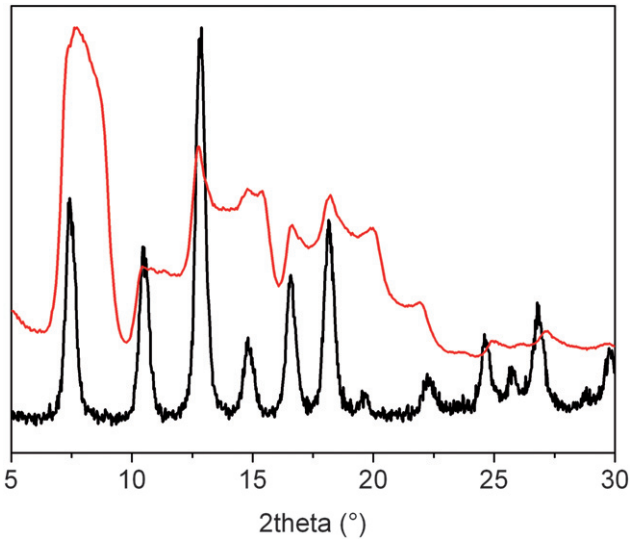

Fig. 1 XRPD pattern of the nanoparticles of ZIF-8 (black) and GI-WAXS on a ZIF-8 thin film (red).

of ZIF-8 with a broadness, in agreement with the presence of small NPs (Fig. 1). To analyse the permanent porosity of the NPs, N_2 adsorption–desorption isotherms were performed at 77 K on ZIF-8 NPs outgassed overnight under dynamic vacuum at 120 °C. This resulted in a surface area of 1696 ± 16 m^2 g^{-1} (BET) and 1904 ± 3 m^2 g^{-1} (Langmuir) (Fig. S3) in good agreement with the value reported for the micrometric ZIF-8 sample, while even surpassing the values reported previously for nanoparticles of ZIF-8. Importantly, this points out the importance of a careful washing step of the particles.

The colloidal solution of ZIF-8 NPs in absolute ethanol is stable for three weeks. However, after one month, the formation of micrometric aggregates is observed. According to the measured positive zeta potential (+ 31 mV) in absolute ethanol, this can be explained through the formation of a hydrogen bonding network between the protonated imidazole molecules at the surface of the particle and the solvent. A partial degradation of the NPs leading to the redispersion of protonated imidazole molecules could also induce the formation of a coordination network between zinc atoms and imidazolate molecules.

Elaboration of the thin films by dip-coating

For a given colloidal solution of a certain concentration and temperature, two phenomena, in addition to solvent evaporation, govern the deposition process. Those two phenomena, namely the draining and capillary regimes, are dependent on the withdrawal speed and directly affect the thickness of the resulting film.[11] At a typical speed (>1 mm s^{-1}), the regime is described with a Landau–Levich model, and the thickness of the cast film increases with the increasing of the withdrawal speed due to the evaporation of the solvent and gravitational draining (viscous drag).[12] At low speed (<1 mm s^{-1}) the film deposition is governed by both interdependent effects of the evaporation and the capillarity, strongly opposing the draining. Consequently, decreasing the speed dramatically increases the film thickness as a result of the interdependence of continuous evaporation of the ethanol solvent at the meniscus and the capillary raise at the drying line "feeding" the deposition already formed.

To tune the thickness of the thin films and the compactness of the NPs, we applied those two regimes. By controlling the speed (from 0.01 to 10 mm s^{-1}) and the colloidal solution concentration (0.2 and 0.02 mol L^{-1}), a single deposition process allowed the production of optical quality films with a wide range of thicknesses (from 40 nm to 1 μm) and different packing of the NPs (Fig. 2). Photos of the deposition of ZIF-8 NPs (Fig. S4) coated at different withdrawal speeds show a color variation dependent on the film thickness and related to the optical interference. The transparency and the high optical transmittance (>96%) of the films (Fig. S5 and S6) point to their homogeneity which can lead to light scattering and they can therefore be regarded as having the high optical quality essential for ellipsometric experiments used in the range of 450–1000 nm. Interestingly, using a colloidal solution of 0.2 mol L^{-1} and by applying the drain regime, the film thickness varied from 161 to 324 nm for a withdrawal speed of 1 to 10 mm s^{-1} (Fig. 2). Slowing down the speed (down to 0.01 mm s^{-1}), while using the capillary regime, led to an optical quality film with a thickness of 1043 nm. This demonstrates that the film is three times thicker than films processed at 10 mm s^{-1}. Using a lower concentration of the colloidal solution (0.02 mol L^{-1}) decreased the film thickness from 497 nm at 0.01 mm s^{-1} (capillary regime) to 89 nm at 10 mm s^{-1} (drain regime), with the lowest being 40 nm at 0.5 mm s^{-1}. Finally, controlling the speed and the concentration is indeed an easy way to tune the thickness of MOF thin films with one unique deposition. With NPs of 28 ± 15 nm in size, it can be suggested that the film thickness of 40 nm produced at 0.5 mm s^{-1} from a 0.02 mol L^{-1} solution corresponds to one ZIF-8 nanoparticulate layer. Meanwhile the deposition of a solution of 0.2 mol L^{-1} at a speed of 0.01 mm s^{-1} leads to a film thickness of 1043 nm corresponding to 40 ± 10 layers of ZIF-8 nanoparticles.

The films were characterized by grazing-incidence wide-angle X-ray scattering (GI-WAXS), ATR-Infra-Red and Field Emission Scanning Electron Microscopy (FE-SEM). The GI-WAXS

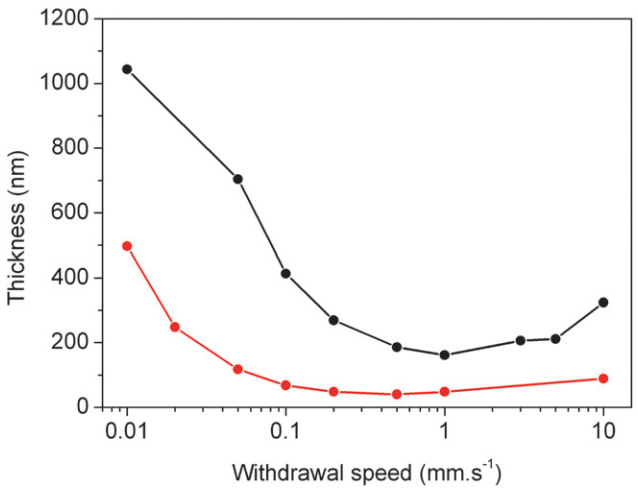

Fig. 2 Effect of the withdrawal speed on the thickness of one deposition of an ethanolic colloidal solution of ZIF-8 with two different concentrations (0.2 mol L^{-1} in black and 0.02 mol L^{-1} in red) performed at room temperature.

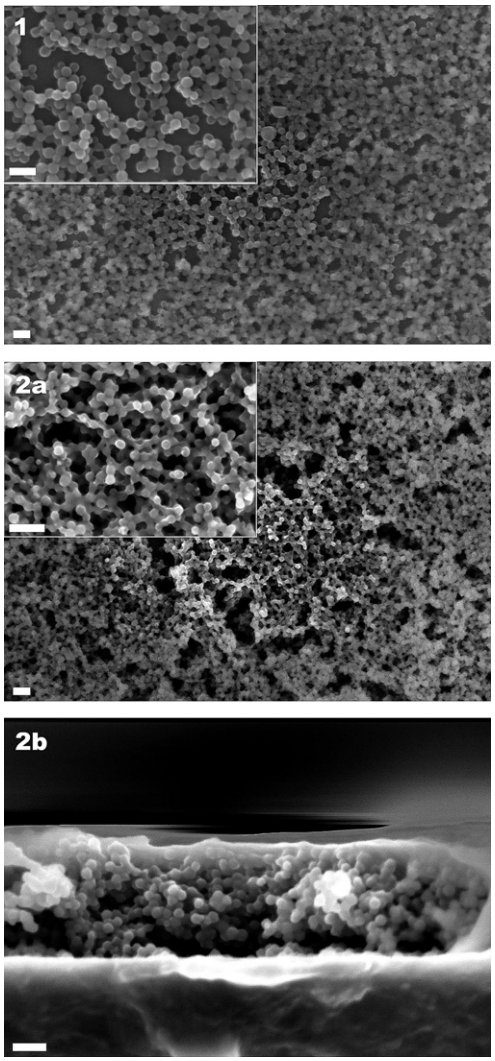

Fig. 3 FE-SEM images of ZIF-8 thin films cast at: 1) 4 mm s^{-1} (top view) and 2) at 0.02 mm s^{-1} (a. top view and b. side view). Scale bar length is 100 nm.

pattern is similar to the XRPD, as well as the infra-red spectrum of the films is close to the one of the ZIF-8 NPs alone, suggesting that the crystalline structure of the MOF is kept when deposited on the silicon wafer (Fig. 1 and S7). The difference in the peak geometry between conventional XRD and GI-WAXS is expected, wherein it is related to the grazing incidence geometry.[13] The FE-SEM pictures of the ZIF-8 thin films cast at 4 and 0.02 mm s^{-1} have thicknesses of 90 and 286 nm (measured by ellipsometry) (Fig. 3). The observed thicknesses of the thin films are in good accordance with the ellipsometric experiments which measures an average. The well-defined microporous ZIF-8 NPs form mesopores, coming from the packing of the NPs and macropores, which may be due to the vacuum applied inside the microscope.

Adsorption of vapors inside the thin films of ZIF-8

To evaluate the influence of the preparation method (capillary and drain regimes) on vapor adsorption, comparative

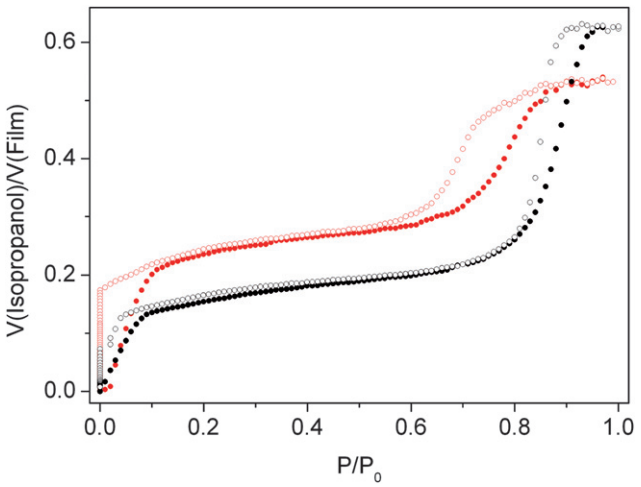

Fig. 4 Environmental ellipsometric isopropanol adsorption at room temperature. In black, on a film made of three successive depositions of ZIF-8 nanoparticles at 5 mm s^{-1} and in red, on a film made of a single deposition of ZIF-8 nanoparticles in a capillarity regime at 0.02 mm s^{-1}. The colloidal solution concentration used for the elaboration of both films is 0.02 mol L^{-1}.

isopropanol adsorption experiments have been carried out at room temperature. The isopropanol adsorption performed by environmental ellipsometry on a film with only one deposition of NPs deposited at 0.02 mm s^{-1} (capillary regime) and a thickness of 286 nm is compared with the one of a film made with three successive depositions at 5 mm s^{-1} (drain regime) and a thickness of 250 nm (Fig. 4). Both curves show a double steps adsorption at low and high relative pressures, this points to a hierarchical pore organization both from the micropores of the ZIF-8 framework and the interparticular mesopores. A representative analysis of the quantity of adsorbed vapors is obtained through the ratio of the volume of adsorbed isopropanol on the volume of the film based on the refractive index of the dense ZIF-8 material (without pores) of 1.54 (Fig. 4). The spectroscopic ellipsometry measurement data have been fitted using a Cauchy model and is in good accordance with the refractive index of reported zinc-based hybrid materials.[14]

Freshly cast thin films obtained in both regimes have refractive indices of 1.18 (made with the fast speed) and 1.23 (made at the ultra slow speed). The difference between the refractive indices suggests a densification of the nanoparticles by decreasing the speed of deposition. This effect of densification of the nanoparticles on the substrate by using the capillary regime is also confirmed by the higher volume, 0.236 cm^3 cm^{-3}, of isopropanol adsorbed at $P/P_0 = 0.2$ for the capillary regime *versus* an isopropanol volume of 0.154 cm^3 cm^{-3} for the film made with a fast withdrawal speed. This shows that the capillarity regime makes it possible to control the thickness but also favors the denser packing of the colloids. The vapor adsorption is also associated with a weak but clearly visible contraction of the film at 1.3 and 1.5% for the films made by drain and capillary regimes, respectively. This may be explained by capillary stresses applied on the ZIF-8 NPs during capillary condensation (Fig. S8 and S9).[10]

At higher relative pressures of isopropanol vapor, the second steep increase in adsorbed alcohol volume is related to the

adsorption of isopropanol molecules within the interparticular mesopores from the film. The volume of these mesopores represents 47.3 and 30.4 vol%, respectively, meaning that the rest of those films are composed of the microporous ZIF-8 NPs (52.7 and 69.6 vol%, respectively). The filling of the interparticular mesopores with isopropanol starts from $P/P_0 = 0.80$ to 0.95 for the film made with three successive layers (drain). The P/P_0 for the single deposition (capillary) was from 0.73 to 0.84. The fact that the adsorption of alcohol starts at lower relative pressures and exhibits a steeper adsorption profile for the film made at slower speeds, is a proof that the capillary regime leads to smaller interparticular mesopores with more narrow size dispersions (pore diameter centered at 14 nm) than the films made with several depositions at a faster speed (pore diameter centered at 25 nm) (Fig. S10). This is also related to the densification of the organisation of NPs induced by the slow capillary regime. Consequently, the capillary regime seems to be more suitable for obtaining a better packing and thus a better distribution of the pores between the particles. The adsorption of isopropanol vapors at high relative pressures is also associated with a contraction of the film thickness (4.3 and 2.0% for the films cast at fast and slow withdrawal speeds, respectively) followed by a steep expansion, pointing to the relaxation of the film due to the complete filling of the pores. The desorption process of isopropanol from the mesopores made by the NPs is fully reversible for both films. The small hysteresis loop observed for both films may be explained by the diffusion restriction occurring in mesoporous materials made by particles. The desorption of isopropanol from the micropores of ZIF-8 shows a hysteresis, wherein a dry flux of air for 10 to 20 min is necessary to desorb all the remaining molecules as a result of the affinity of OH groups within the pores of ZIF-8. To test the reversibility of the isopropanol adsorption process in ZIF-8 micropores and the robustness of the films, a dynamic environmental ellipsometric analysis has been carried out with repetitive cycling of 60% isopropanol saturation pressures in air followed by dry air at 25 °C (Fig. 5). A change of the refractive index from 1.16 to 1.24 is observed upon adsorption of isopropanol vapors within 20 s, highlighting the fast filling of the micropores with alcohol. Even if the complete desorption process needs 20 min, desorption of 50% of the pores takes only a few minutes. The filling/draining of the half-filled pores of ZIF-8 is fully reproducible over repeated cycles, indicating that the material is able to withstand cyclic exposure to the vapor stream. Significantly, the isopropanol ability to adsorb on a ZIF-8 thin film is maintained over repeated cycling, and the material can be easily regenerated by switching the vapor stream to air. This may render the material suitable for use as sensors or vapor detectors.

To study the adsorption properties of the thin films of ZIF-8, we carried out environmental ellipsometry experiments with other solvents with different sizes and polarities such as water, THF, n-heptane, iso-octane, cyclohexane and toluene (Fig. 6). The water adsorption isotherm at room temperature on bulk material has already been reported as showing the absence of adsorption related to the strong hydrophobic characteristics of ZIF-8, as a consequence of the presence of methyl groups positioned at the entrance of the pore opening.[15] Cast on a silicon substrate, the NPs of ZIF-8 maintain the hydrophobic character, showing no significant adsorption of water below $P/P_0 = 0.8$. From this relative pressure, the steep increase to a refractive index of 1.31 is due to some water condensation resulting in a pore volume of 64% of the film. This high value means that at high relative pressures, the water partially fills the micropores of the ZIF-8 and the mesopores formed by the interparticle voids.[16] To test the possibility of the ZIF-8 thin films to adsorb aprotic polar solvents, we have measured the adsorption isotherm of THF. The sharply increasing adsorption curve occurring at very low pressures ($P/P_0 = 0.01$) confirms the high affinity of the micropores of the ZIF-8 towards the THF vapors. Note that the mesopores of the film are continuously filled with THF starting from $P/P_0 = 0.01$ to 1. This can be explained by the low boiling point and high vapor pressure of THF. Concerning the adsorption of hydrocarbons, the diffusion rate and the quantity of adsorbed molecules are dependent on the size of the guest, resulting in the following order of affinity from linear chains

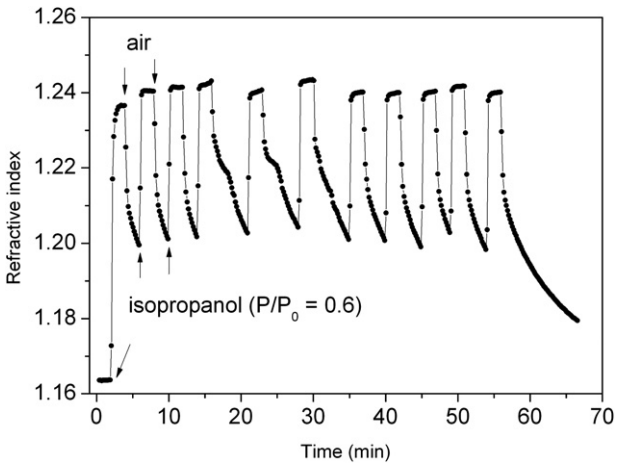

Fig. 5 Isopropanol vapor cycling ellipsometric experiment on a ZIF-8 thin film at 25 °C, employing a flow of $P/P_{vapsat} = 60\%$ of isopropanol in air followed by a flow of pure air.

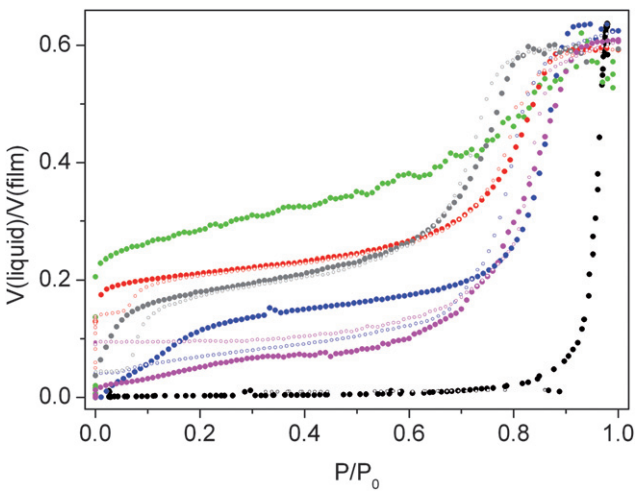

Fig. 6 Evolution of sorbed liquid volume (filled circles) of ZIF-8 film during water (black), THF (green), n-heptane (red), iso-octane (grey), cyclohexane (blue) and toluene (pink) adsorption (full circles) and desorption (empty circles) isotherms at room temperature.

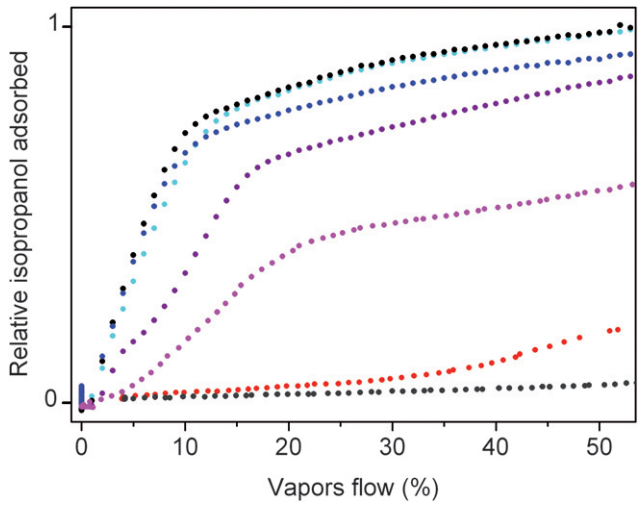

Fig. 7 Environmental ellipsometric experiments on a ZIF-8 thin film upon isopropanol vapor adsorption from an isopropanol/water mixture. In black at 100%, cyan at 27%, blue at 12%, purple at 5%, pink at 1%, red at 0.1% and grey at 0% of isopropanol in water (by volume).

(n-heptane, at $P/P_0 = 0.03$) > branched chains (iso-octane, at $P/P_0 = 0.1$) > non-aromatic ring (cyclohexane, at $P/P_0 = 0.25$) $\gg$ aromatic ring (toluene, at $P/P_0 = 0.35$), this last one being almost not adsorbed at all. This series show the affinity of ZIF-8 with hydrocarbons and make the films good candidates for hydrocarbons size selective separation, coupled with its hydrophobic character.

Finally, to test the ability of the thin films of ZIF-8 as a vapor sensor, environmental ellipsometric experiments with different loadings of isopropanol in water have been carried out. To control the vapor flow, dry and humid air flows are mixed in the chamber of the ellipsometer. The flow rate is controlled by a mass flow controller with a maximum rate of 5 mL L^{-1}. For each experiment, a total volume of one litre solution of isopropanol/water is freshly prepared, and the controlled bubbling inside the solution constituted a humidified flow. In Fig. 7, at 100% of isopropanol and at 27%vol of isopropanol in water, the adsorption of alcohol is at its maximum, meaning that there is a total separation of alcohol from water at 55% of vapor flow. With up to 1%vol of isopropanol content in water, the film still exhibits an adsorption isotherm. This demonstrates a good efficiency of the system for alcohol adsorption. The decrease in the quantity of adsorbed molecules may be explained by the lower loading of alcohol in the mixture. At 0.1%vol of isopropanol in solution, the film does not adsorb any more, showing the limit of the separation from the system and/or the limit of the experiment setup. This separation capability of the ZIF-8 thin films of isopropanol/water up to 1%vol of alcohol surpasses classical distillation techniques, and may break the azeotrope formed by the two liquids.

Conclusions

The preparation from a stable colloidal solution of ZIF-8 NPs (28 ± 15 nm) allows the processing of thin films of high optical quality by dip-coating. The control of the density and the thickness of thin films of the ZIF-8 can be tailored from 40 nm to 1 μm by using the drain and capillary regimes coupled with different NP concentrations. Remarkably, a thick film can be formed in the capillary regime with a single deposition of a low concentration of NPs.

Through environmental ellipsometric porosimetry, the adsorption properties of the porous thin films of ZIF-8 have been characterized. The pores of ZIF-8 are hydrophobic which explains why only organic molecules such as alcohols, THF and hydrocarbons are adsorbed. The ZIF-8 films possess a dual hierarchical structure of micro/mesopores for an easier accessibility and faster diffusion rate of molecules. Finally, these thin films exhibit both a good robustness upon several cycles of alcohol adsorption and potential selective adsorption properties for organic vapors *versus* water which could make those high optical thin films good candidates as sensors for vapor or separative membranes.

Acknowledgements

The authors thank M. Selmane for WAXS experiments and P. Le Griel for the TEM images. Work partially funded by ANPCyT (PICT 34518, PAE 2006 37063-00038). AD would like to acknowledge C'Nano IdF for her project funding and the ECOS-Sud agency (A08E05) for travel funds. GJAASI is a member of CONICET

References

1 Themed issue: Metal–organic frameworks, J. R. Long and O. M. Yaghi, *Chem. Soc. Rev.*, 2009, p. 1201–1508; G. Férey, *Chem. Soc. Rev.*, 2008, **37**, 191.
2 S. Hermes, F. Schröder, R. Chelmowski, C. Wöll and R. A. Fischer, *J. Am. Chem. Soc.*, 2005, **127**, 13744; D. Zacher, O. Shekhah, C. Wöll and R. A. Fischer, *Chem. Soc. Rev.*, 2009, **38**, 1418.
3 J. Gascon, S. Aguado and F. Kapteijn, *Microporous Mesoporous Mater.*, 2008, **113**, 132.
4 Y.-S. Li, F.-Y. Liang, H. Bux, A. Feldhoff, W.-S. Yang and J. Caro, *Angew. Chem. Int. Ed.*, 2010, **49**, 548.
5 O. Shekhah, H. Wang, D. Zacher, R. A. Fischer and C. Wöll, *Angew. Chem., Int. Ed.*, 2009, **48**, 5038.
6 A. Demessence, P. Horcajada, C. Serre, C. Boissière, D. Grosso, C. Sanchez and G. Férey, *Chem. Commun.*, 2009, 7149; P. Horcajada, C. Serre, D. Grosso, C. Boissière, S. Perruchas, C. Sanchez and G. Férey, *Adv. Mater.*, 2009, **21**, 1931.
7 K. S. Park, Z. Ni, A. P. Côté, J. Y. Choi, R. Huang, F. J. Uribe-Romo, H. K. Chae, M. O'Keeffe and O. M. Yaghi, *Proc. Natl. Acad. Sci. U. S. A.*, 2006, **103**, 10186.
8 H. Bux, F. Liang, Y. Li, J. Cravillon, M. Wiebcke and J. Caro, *J. Am. Chem. Soc.*, 2009, **131**, 16000.
9 J. Cravillon, S. Münzer, S.-J. Lohmeier, A. Feldhoff, K. Huber and M. Wiebcke, *Chem. Mater.*, 2009, **21**, 1410.
10 C. Boissière, D. Grosso, S. Lepoutre, L. Nicole, A. Brunet Bruneau and C. Sanchez, *Langmuir*, 2005, **21**, 12362.
11 M. Le Berre, Y. Chen and D. Baigl, *Langmuir*, 2009, **25**, 2554; M. Faustini, B. Louis, P. A. Albouy, M. Kuemmel and D. Grosso, *J. Phys. Chem. C*, 2010, **114**, 7637.
12 C. J. Brinker, G. C. Frye, A. J. Hurd and C. S. Ashley, *Thin Solid Films*, 1991, **201**, 97.
13 M. Faustini, L. Nicole, C. Boissière, P. Innocenzi, C. Sanchez and D. Grosso, *Chem. Mater.*, DOI: 10.1002/cm100937e.
14 Q. Peng, B. Gong, R. M. VanGundy and G. N. Parsons, *Chem. Mater.*, 2009, **21**, 820.
15 P. Küsgens, M. Rose, I. Senkovska, H. Fröde, A. Henschel, S. Siegle and S. Kaskel, *Microporous Mesoporous Mater.*, 2009, **120**, 325.
16 C. E. Ramachandran, S. Chempath, L. J. Broadbelt and R. Q. Snurr, *Microporous Mesoporous Mater.*, 2006, **90**, 293.

